Alginate@TiO_2 hybrid microcapsules with high in vivo biocompatibility and stability for cell therapy

Leroux, Grégory; Neumann, Myriam; Meunier, Christophe F.; Voisin, Virginie; Habsch, Isabelle; Caron, Nathalie; Michiels, Carine; Wang, Li; Su, Bao Lian

Published in:
Colloids and Surfaces B: Biointerfaces

DOI:
10.1016/j.colsurfb.2021.111770

Publication date:
2021

Document Version
Version created as part of publication process; publisher's layout; not normally made publicly available

Journal Pre-proof

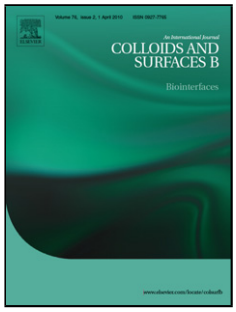

Alginate@TiO_2 Hybrid Microcapsules with High *In Vivo* Biocompatibility and Stability for Cell Therapy

Grégory Leroux (Conceptualization) (Methodology) (Validation) (Investigation) (Writing - original draft), Myriam Neumann (Formal analysis) (Validation) (Writing - original draft), Christophe F. Meunier (Methodology) (Formal analysis) (Investigation), Virginie Voisin (Investigation) (Validation), Isabelle Habsch (Investigation) (Validation), Nathalie Caron (Resources), Carine Michiels (Resources) (Supervision), Li Wang (Investigation) (Formal analysis) (Writing - original draft) (Writing - review and editing) (Visualization), Bao-Lian Su (Conceptualization) (Writing - review and editing) (Project administration)

PII: S0927-7765(21)00214-9

DOI: https://doi.org/10.1016/j.colsurfb.2021.111770

Reference: COLSUB 111770

To appear in: *Colloids and Surfaces B: Biointerfaces*

Received Date: 22 October 2020

Revised Date: 7 April 2021

Accepted Date: 14 April 2021

Please cite this article as: Leroux G, Neumann M, Meunier CF, Voisin V, Habsch I, Caron N, Michiels C, Wang L, Su B-Lian, Alginate@TiO_2 Hybrid Microcapsules with High *In Vivo* Biocompatibility and Stability for Cell Therapy, *Colloids and Surfaces B: Biointerfaces* (2021), doi: https://doi.org/10.1016/j.colsurfb.2021.111770

Alginate@TiO_2 Hybrid Microcapsules with High *In Vivo* Biocompatibility and Stability for Cell Therapy

Grégory Leroux,[§,$] Myriam Neumann,,[§,$] Christophe F. Meunier,[§, $] Virginie Voisin,[‡] Isabelle Habsch,[‡] Nathalie Caron,[‡] Carine Michiels,[#] Li Wang[§,$,+,] and Bao-Lian Su[§,$,¶,*]*

[§]Laboratory of Inorganic Materials Chemistry (CMI), University of Namur, 61 Rue de Bruxelles, B-5000 Namur, Belgium.

[$]Namur Institute of Structured Matter (NISM), University of Namur, 61 Rue de Bruxelles, B-5000 Namur, Belgium.

[‡]Molecular Physiology Research Unit (URPhyM), Namur Research Institute for Life Sciences (NARILIS), University of Namur, 61 Rue de Bruxelles, B-5000 Namur.

[#]Laboratory of Biochemistry and Cell Biology (URBC), Namur Research Institute for Life Sciences (NARILIS), University of Namur, 61 Rue de Bruxelles, B-5000 Namur.

[¶]State Key Laboratory of Advanced Technology for Materials Synthesis and Processing, Wuhan University of technology, Luoshi Road 122, Wuhan 430070, China.

[+]Current address: Materia Nova R&D Center, Avenue du champ de Mars 6, 7000 Mons, Belgium.

Corresponding Authors

*E-mail: li.wang@materianova.be (L. Wang)

*E-mail: bao-lian.su@unamur.be (B. L. Su)

Graphical abstract

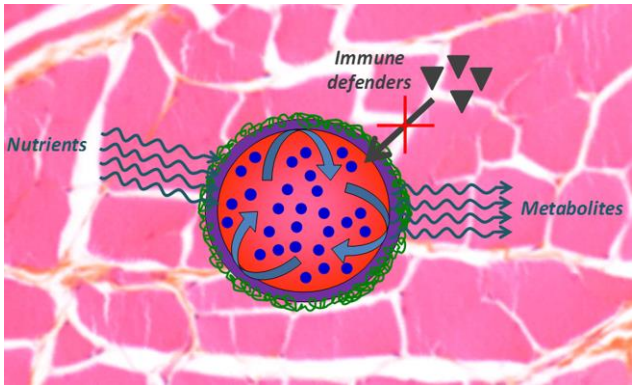

Highlights

- Alginate@TiO_2 hybrid microcapsules are designed for cell encapsulation towards cell therapy
- Alginate@TiO_2 hybrid microcapsules show high *in vivo* stability
- Alginate@TiO_2 hybrid microcapsules demonstrate high biocompatibility
- Alginate@TiO_2 hybrid microcapsules provide entrapped cells with immune isolation

STATISTICAL SUMMARY: This article contains 8484 number of words, 1 schematic diagram, 6 figures and 1 table.

ABSTRACT: Designing new materials to encapsulate living therapeutic cells for the treatment of the diseases caused by protein or hormone deficiencies is a great challenge. The desired materials need to be biocompatible towards both entrapped cells and host organisms, have long-term *in vivo* stability after implantation, allow the diffusion of nutrients and metabolites, and ensure perfect immune-isolation. The current work investigates the *in vivo* biocompatibility and stability of alginate@TiO_2 hybrid microcapsules and the immune-isolation of entrapped HepG2 cells, to assess their potential for cell therapy. A comparison was made with alginate-silica hybrid microcapsules (ASA). These two hybrid microcapsules are implanted subcutaneously in female Wistar rats. The inflammatory responses of the rats are monitored by the histological examination of the implants and the surrounding tissues, to indicate their *in vivo* biocompatibility towards the hosts. The *in vivo* stability of the microcapsules is evaluated by the recovery rate of the intact microcapsules after implantation. The immune-isolation of the entrapped cells is assessed by their morphology, membrane integrity and intracellular enzymatic activity. The results show high viability of the entrapped cells and insignificant inflammation of the hosts, suggesting the excellent biocompatibility of alginate@TiO_2 and ASA microcapsules towards both host organisms and entrapped cells. Compared to the ASA microcapsules, more intact alginate@TiO_2 hybrid microcapsules are recovered 2-day and 2-month post-implantation and more cells remain alive, proving their better *in vivo* biocompability, stability, and immune-isolation. The present study demonstrates that the alginate@TiO_2 hybrid microcapsule is a highly promising implantation material for cell therapy.

KEYWORDS: Hybrid hydrogels, cell encapsulation, *in vivo* biocompatibility, *in vivo* stability, immune isolation

1. INTRODUCTION

Cell therapy refers to the *in vivo* transplantation of living therapeutic cells to functionally substitute original dysfunctional tissues or organs, aiming at treating the diseases caused by protein or hormone deficiencies.[1-2] It is considered as an emerging and very important medical approach to address the limited supply of donors for therapy. However, this treatment often suffers from failure by the low viability and activity of the implanted cells under the immune attack and the inefficient oxygen and nutrient supplementation.[3-6] Cell encapsulation, a technology to entrap living cells in materials, has been evolved to be a very important field of current interest and demonstrates promising perspectives in a large range of applications, including biosensors, biocatalysis, bioproduction, and medicine.[7-10] Materials with controlled semi-permeability have been considered as an excellent matrix to encapsulate cells for cell therapy, because they not only can protect therapeutic cells from immune attacks, but also permit the incoming of oxygen and nutrients and the outgoing of metabolic products and molecules of interest (e.g. insulin for treatment of *diabetes mellitus*), thus maximally persevering the therapeutic effect of the entrapped cells.[11-13] The materials designed for therapeutic cell encapsulation should be biocompatible to the entrapped cells to maintain their high viability, as well as to the host organisms to avoid inflammation or even rejection of the implants.[14] In addition, the designed materials should be chemically inert to the implantation environment and high *in vivo* mechanically stable with good elasticity and deformability, thus not only ensuring the long-term functioning of the entrapped cells but also enabling to resist the sudden pressure changes due to body movement. Such designed materials could serve as artificial organs for the replacement of defective organs and the treatment of the diseases caused by hormone deficiencies (such as the increasingly widespread type 1 *diabetes mellitus*).[15-16]

Hydrogels, owing to their various compositions, tunable nanostructure, tailorable properties and multiple functionalization ability, have shown great potential in bioengineering and medicine.[17-19] Alginate-based microcapsule is one of the most-used hydrogels for cell encapsulation, because of their high biocompatibility, low cost, and mild gelation properties.[20-21] However, pure alginate hydrogels usually suffer from low chemical stability, low mechanical strength and uncontrollable diffusion of substances, which leads to poor cell protection and preservation when applied in cell therapy. Inorganic gels, such as silica and titania, have been reported in cell encapsulation to replace alginate hydrogels.[22-24] Compared to alginate-based hydrogels, inorganic gels present higher chemical stability, enhanced mechanical properties, and well controlled porosity, contributing to their long-term stability and thus providing the encapsulated cells with excellent protection.[25-26] Nevertheless, some by-products generated during the formation of inorganic gels, such as short chain alcohols from their alkoxy precursors or salts from their aqueous precursors like Na_2SiO_3, have harmful effects on the viability and activity of encapsulated cells, thus decreasing the therapeutic effects of these cell-laden inorganic gels.[27] The direct contact between inorganic compounds and encapsulated cells would lead to the change of cell configuration, thus negatively influencing the cell viability and activity.[28-31] In addition, the direct contact between pure solid inorganic matrix, in spite of their good biocompatibility, and host organism could induce inflammation due to the friction, thus leading to the rejection of cell-laden pure inorganic matrix.[29] Hybrid hydrogels on the basis of the combination of hydrogels and inorganic compounds have been demonstrated to address the above mentioned problems.[32-34] For example, alginate-silica microcapsules in which a silica layer was deposited on an alginate sphere were designed to encapsulate microalgae cells and animal cells.[35] Such microcapsules demonstrated excellent biocompatibility, improved mechanical strength, and well-adapted porosity, thus providing the encapsulated cells with a

biocompatible and stable microenvironment for their long-term viability and activity towards photosynthetic production or cell therapy.[36-40] However, the slow *in vivo* dissolution of silica was observed when this hybrid hydrogel was implanted in the body of rats, meanwhile silica was reported to attract macrophages to induce oxidative stress and pro-inflammatory responses, thus limiting their effects in cell therapy *in vivo*.[40] Most recently, alginate@TiO_2 microcapsules were reported to be a very promising material to encapsulate animal cells[41] such as insulin-secreting cells[42] in cell therapy. This microcapsule was formed in a mild reaction condition and showed high biocompatibility, enhanced chemical and mechanical stability and well-controlled porosity.[41] On the basis of the *in vitro* study, such hybrid microcapsule can serve as a favorable cell reservoir. The encapsulated cells presented long-term viability (43 days for the encapsulated HepG2 cells)[41] and the constant release of metabolic products[41] and insulin[42], demonstrating the great potential of the alginate@TiO_2 microcapsules in the treatment of several sever diseases especially Type 1 *diabetes mellitus*[42]. In addition, the immune responses elicited by titanium or TiO_2 implants are of a hot research topic in the field of immunology and medicine. Titanium implants in bone could activate the immune system and suppress bone resorption, thus offering a favorable bone forming environment after their implantation.[43] Furthermore, TiO_2 could give rise to oxidative stress and pro-inflammatory responses[44], whereas the elicited pro-inflammation could be recovered in a short time due to the rapid phenotype switch of macrophages from M1 (inflammatory macrophages) to M2 (anti-inflammatory macrophages) induced by TiO_2[45]. Therefore, investigating the *in vivo* behavior of the alginate@TiO_2 hybrid microcapsules could be highly beneficial on both practical cell therapy and fundamental immunology.

We herein present the *in vivo* performance of the alginate@TiO_2 hybrid microcapsules without or with encapsulated cells, in order to assess the potential of these cell-laden hydrogels in practical clinical cell therapy. The microcapsules were synthesized based on our

previous well controlled and biocompatible protocol.[41-42] The core of such microcapsules is the alginate-based hydrogel which is formed by the cross-linking of alginate and calcium ions, while the shell is mainly composed of titania which is formed by the polycation-induced hydrolysis and condensation of a biocompatible precursor (titanium(IV) bis(ammonium lactato)dihydroxide (TiBALDH)). An *in vivo* behavior comparison was made between alginate@TiO_2 hybrid microcapsules and alginate-silica-alginate (ASA) hybrid microcapsules.[37, 40] The ASA microcapsules were set as a control in this study instead of pure alginate microcapsules, because the animal cells entrapped in ASA microcaspules had showed much better long-term viability and activity than that entrapped in pure alginate microcapsules.[37] Human hepatocellular carcinoma cells (HepG2) have been used as model cells for cell encapsulation because of their fast proliferation, their similarity with β-cells in terms of size and shape, their continuous secretion of albumin. The studies on HepG2 cells could be very beneficial to the further deep investigation of cell-laden hydrogels for the possible clinical cell therapy on *diabetes mellitus*. The morphology, structure and chemical composition of the microcapsules were first characterized in detail. The *in vivo* stability of the microcapsules was evaluated by the morphology maintenance and the recovery rate of the intact microcapsules 2 days and 2 months after implantation. The *in vivo* biocompatibility of the microcapsules to both the encapsulated cells and the host organisms were carefully investigated by observing their morphology change after implantation, by monitoring the weight change of the transplanted rats, and by analyzing the implants and the surrounding tissues of the transplanted rats. The very important property on the immune-isolation of the microcapsules was assessed by tracing the viability and the morphology change of the entrapped cells after implantation.

2. EXPERIMENTAL

Chemical materials. Alginic acid sodium salt from brown algae (for immobilization of microorganisms), calcium chloride (dihydrate, 99%), titanium(IV) bis(ammonium lactato)dihydroxide solution (TiBALDH, 50 wt.% in H_2O), poly(diallyldimethylammonium) chloride solution (PDDAC, 20 wt.% in H_2O), ethylene glycol-bis(β-aminoethyl ether)-N, N, N', N'-tetraacetic acid (EGTA, tetrasodium salt, 97%), hydrochloric acid (Molecular Biology Grade, 36.5-38.0%), sodium hydroxide (reagent grade, 98%, anhydrous), chloroform (anhydrous, 99%), glutaraldehyde (50 wt. % in H_2O), and fluorescein diacetate (FDA, used as a cell viability dye) were purchased from Sigma-Aldrich. Sodium silicate (extra pure, assay (acidimetric, SiO_2) 25.5-28.5 %) was purchased from Merck. Ethanol (absolute) were purchased from Fisher. Phosphate Buffered Saline (PBS, 0.0067 M (PO_4), For Cell Culture) was supplied by Lonza. Dulbelcco's Modified Eagle Medium (DMEM, 31885) and foetal bovine serum (FBS) were provided from Invitrogen (Casbald, USA).

Sodium alginate powder was purified as described by de Vos *et al.*[46], in order to remove Mg^{2+} and Ca^{2+} cations, and some proteins which would influence the viabiliaty and activity of the encapsulated cells.

Biological materials. HepG2 cells (Hepatocellular Liver Carcinoma Cell line) were purchased from the American Type Culture Collection (ATCC HB-8065) and cultivated in Dulbelcco's Modified Eagle Medium (DMEM, 31885) supplemented with 10% of foetal bovine serum in 75-cm^2 flasks (Costar, Lowell, USA). The cells were incubated at 37 °C (95% air / 5% CO_2) for three days. Subsequently, the cells were washed with PBS, treated with a trypsin/EDTA mix, centrifuged (1000 rpm for 5 min), collected and then resuspended in fresh culture medium for encapsulation.

Synthesis of hybrid microcapsules. The encapsulation of HepG2 cells in alginate/titania microcapsules (alginate@TiO_2) and in alginate-silica/alginate microcapsules (ASA) was performed from the same batch of cells and with the same purified alginate solution. The

final cell density in alginate@TiO_2 microcapsules and in ASA microcapsules was $2.2*10^6$ cells mL^{-1}.

Cell encapsulation in alginate@TiO_2 microcapsules. The microcapsules were obtained through the procedure presented in Scheme 1A.[41] First, HepG2 cells were collected in a fresh buffered culture medium and mixed with purified sodium alginate (3.0 *wt.*%). A buffered titanium precursor solution diluted in the culture medium without serum was added to cell-alginate mixture with a volume ratio of 1:1. The obtained mixture was homogenized by aspiration with a disposable transfer pipet and then directly extruded into a buffered aqueous solution containing calcium chloride (100 mM) and PDDAC (0.4 *wt.*%) at a rate of about 1 drop per second. The drops in aqueous solition containing calcium chloride were transformed into microcapsules. After 5 min of incubation, all the microcapsules were covered with a white solid crust, indicating that a reaction occurred between the titania precursor (TiBALDH) and PDDAC. The hybrid microcapsules were then harvested, stored in test tubes filled with 5.0 mL of fresh culture medium and cultured at 37 °C for 4 days before implantation. The diameter of the alginate@TiO_2 microcapsules is 2.76 ± 0.15 mm.

Cell encapsulation in ASA microcapsules. The microcapsules were formed using the procedure presented in Scheme 1B.[37] First, HepG2 cells collected in fresh culture medium were mixed with a sodium alginate (3.0 *wt.*%). This mixture was extruded into a calcium chloride solution (100 mM) using a disposable transfer pipet and alginate microcapsules were formed. After 5 min of incubation, these microcapsules were then transferred in a sodium silicate solution (1.5 M) for 1 min, for the formation of alginate-silica microcapsules. Finally, an external crust of calcium alginate was formed around the microcapsules by immerging them in a fresh buffered sodium alginate solution (1.5 *wt.*%) and next in a calcium chloride solution (110 mM) for 5 min. The formed ASA microcapsules were collected and stored in

test tubes filled with 5.0 mL of fresh culture medium and maintained at 37 °C for 4 days before implantation. The diameter of the ASA microcapsules is 2.67 ± 0.14 mm.

Animal experiments.

Ethics statement. The present work fulfills the statements of the National Institutes of Health Guide for the Care and Use of Laboratory Animals and the project was validated by the Committee on the Ethics of Animal Experiments of the University of Namur (Record Number: FUNDP AR 10/136).

Animals. The first series of experiments were performed on 16 weeks old female Wistar rats bred in our animal facility under controlled environmental conditions. The second series of experiments were performed on 11 weeks old female Wistar rats purchased from Harlan. The animals were fed with a standard rat food diet and had free access to water. They were housed 2 per type III/H cage with an enriched environment.

Surgical procedure. First, anesthesia was performed on animals by an intraperitoneal injection of a mix of ketamine and xylazine (2 mL kg^{-1} of a ketamine (100 mg mL^{-1}) and xylazine (200 mg mL^{-1}) isotonic saline solution) using a 25G needle. They were then placed on a heated table maintaining a constant body temperature of 37°C. Perioperative analgesia was also administrated (injection of a 20 mg mL^{-1} buprenorphine isotonic saline solution in an amount of 500 µL kg^{-1}). A 1 cm skin incision was performed along the back midline located between the shoulder blades. After the blunt dissection of tissue, three microcapsules were implanted subcutaneously on each side of the incision, which was closed using absorbable 4-0 Ethicon Vicryl suture thread. The rats were then allowed to recover under a heat lamp. During all the experiments, the animals were daily examined in order to evaluate their welfare. Various parameters were considered such as their rodent habits, their behavior to detect prospective anxiety or discomfort, their feeding and their weight. The inflammation potentially induced by implanted materials was assessed by identifying surgical site irritation

or scratching. If any inflammation was detected, a local antiseptic treatment was applied (Astrexine powder, chlorhexidin hydrochlorid, supplied by Pierre Fabre, France). At the end of the experiments, animals were euthanized with an intraperitoneal injection of Nembutal (200 mg kg^{-1}, 25G needle) followed by a cervical dislocation. For the second experiment, the rats were first anesthetized before euthanasia, according to the protocol described above, in order to take blood samples for the assessment of the direct inflammatory response by quantifying IL-6 concentration in plasma. The blood sampling was performed by intracardiac puncture using a 23G needle. After euthanasia, microcapsules were first collected for characterization. Afterwards, surrounding tissues were sampled in order to assess local inflammation.

Experimental groups. For each series of experiments, three groups were considered:

Alginate@TiO_2 microcapsule group. This group was divided in two subgroups. In the first one, blank microcapsules without HepG2 cells were implanted in rats (TiO_2 subgroup, n=5 for each experiment). In the second one, rats were implanted with microcapsules with encapsulated HepG2 cells (TiO_2-Cells subgroup, n=5 for each experiment).

ASA microcapsule group. This group was also divided in two subgroups, in the same manner as alginate@TiO_2 microcapsule group. The first one included rats implanted with blank microcapsules without entrapped HepG2 cells (ASA subgroup, n=5 for each experiment) and the second one was composed of rats with HepG2 cell containing implants (ASA-Cells subgroup, n=5 for first experiment, n=6 for second experiment).

Control group (n=5 for the first experiment, n=8 for the second experiment). Rats underwent anesthesia and surgery without microcapsule implantation.

Characterization techniques.

Material properties. Alginate@TiO_2 and ASA microcapsules were dehydrated with ethanol and dried through a process of critical point drying with liquid carbon dioxide in

order to avoid the structural collapse of the microcapsules. Implants collected after the euthanasia of rats were first fixed in a glutaraldehyde solution (3.0 *wt.*%) and subsequently treated through the same drying process. The morphology was observed using field emission scanning electron microscopy (FE-SEM) (JEOL JSM-7500F, Japan). Prior to observation, the samples were sputter-coated with gold. The chemical composition of the samples was evaluated using an energy-dispersive X-ray (EDX) analysis system with an acceleration voltage of 15.00 kV and a working distance of 8 mm.

Cell viability. The intracellular enzymatic activity of encapsulated cells was assessed using a vital dye staining (fluorescein diacetate, FDA). Encapsulated cells were incubated within a diluted FDA solution (5 µM, in culture medium) for 5 min at room temperature. Micrographs were taken using a fluorescent Multizoom AZ100 microscope (Nikon, Japan) with a bright-field mode or a 482(±35) nm/536(±40) nm excitation/emission light.

Histological staining. Tissues and collected microcapsules were fixed in Duboscq-Brazil fluid for 48 h, then transferred into baths of ethanol, butanol and paraffin. The samples were embedded in paraffin, cut into 6 µm sections and stained following the HES (Haematoxolyn-Eosin-Safranin) protocol before histological examination. Briefly, the trichromic stain was applied by passing the microscope slides successively through baths of toluene, methanol, water, haematoxylin, water, hydrochloric acid supplemented with ethanol, water, eosin, water, ethanol, isopropanol, safranin, isopropanol and toluene (automated stainer COT 20 manufactured by Medite, Inc). A mixture of distyrene, a plasticiser (tricresyl phosphate) and Xylene (DPX) was used to attach coverslips to the slides. The histological observation of tissue was carried out using a Multizoom AZ100 microscope (Nikon, Japan) with a DS-Ri1 camera in bright-field mode.

ELISA. The quantity of IL-6 in plasma samples was determined using an ELISA kit (RayBio Rat IL-6 ELISA Kit, RayBiotech, Inc.). Plasma samples were collected by putting

blood samples in 5 mL test tubes supplemented with 0.4 mL of citrate buffer (Venoject, Terumo) and centrifuged immediately at 2500 rpm for 10 min. Supernatant was collected and stored in eppendorf at -80°C.

The quantity of MCP-1 in tissue lysates was determined using a MCP-1 ELISA kit (RayBiotech, Inc.). The collected muscle samples, stored at -80 °C, were firstly lysed in PBS using a tissue homogenizer. The quantity of total proteins in tissue lysate was assessed using a dye reagent (Bio-Rad Protein Assay) and by measuring the absorbance at 595 nm. The measured concentration of MCP-1 was normalized per mg of total proteins in a tissue lysate sample.

Statistical analysis. Statistical analysis was performed to compare IL-6 and MCP-1 concentration data of Wistar rats with and without implants. The non-parametric two-tailed Mann-Whitney U test was applied. Less than 0.05 of *p*-value was considered as significant. These analyses were performed using XLSTAT 2013 software (Addinsoft).

3. RESULTS AND DISCUSSION

Synthesis and characterization of microcapsules. The synthesis procedures of alginate@TiO_2 and ASA microcapsules are presented in Scheme 1A and 1B, respectively. Both microcapsules are mainly composed of alginate in their core. The titania shells of alginate@TiO_2 microcapsules are formed through the hydrolysis and condensation of TiBALDH, while the silica shells of ASA microcapsules are synthesized through the acidification of sodium silicate. Both formation processes have been evidenced to be biocompatible according to the cytotoxicity test of their reaction precursors, products, and by-products.[37, 41] Importantly, the pore size of alginate@TiO_2 and ASA microcapsules can be tuned in order to allow an easy diffusion of nutrients and secreted metabolites and

simoultaneous immune-isolation. This semi-permeability with well controlled porosity makes these microcapsules very promising cell reservoirs for cell therapy.[37, 41]

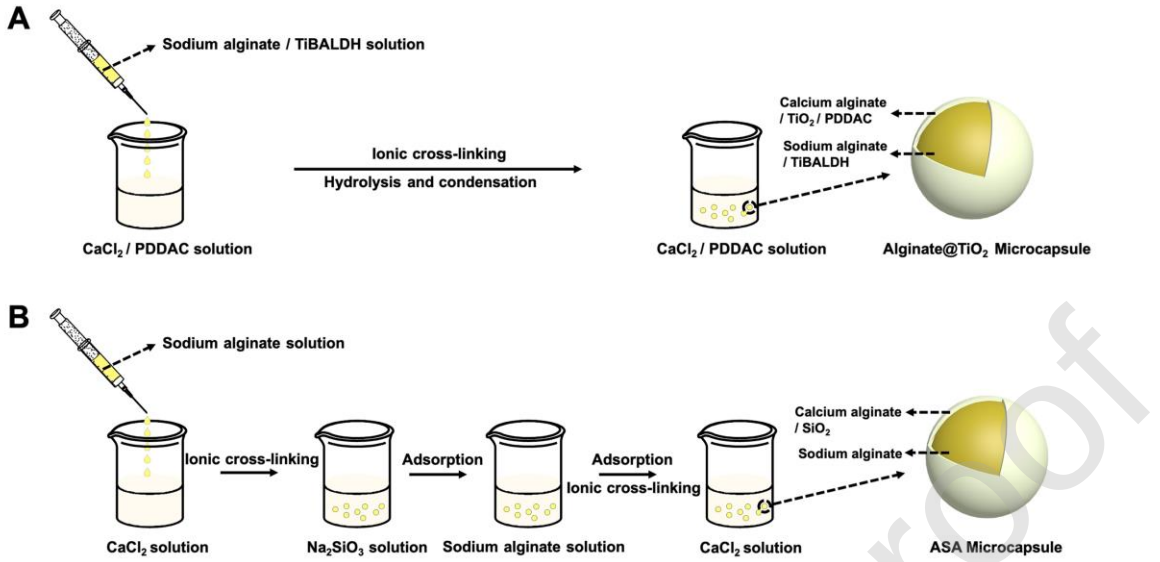

Scheme 1. Synthesis of the alginate@TiO_2 and the ASA microcapsules. (A) Fabrication procedure of alginate@TiO_2 microcapsules. The mixture of sodium alginate and TiBALDH is dropped into a solution of calcium chloride and PDDAC to form alginate@TiO_2 hybrid microcapsules through the ionic crossing-linking of alginate and the hydrolysis and condensation of TiBALDH. (B) Fabrication procedure of ASA microcapsules. A sodium alginate solution is dropped into a solution of calcium chloride to form alginate microcapsules through the ionic crossing-linking of alginate. Subsequently, the formed microcapsules are incubated into a sodium silicate, sodium alginate and calcium chloride solution step by step to form ASA microcapsules through the absorption and ionic crossing-linking processes.

SEM micrographs of both ASA (Figure 1A) and alginate@TiO_2 (Figure 1B) microcapsules present spherical morphology. The surface of the ASA microcapsule is quite smooth, while deep wrinkles but no cracks can be observed on the surface of the alginate@TiO_2 microcapsules. The appearance of deep wrinkles on the surface of the alginate@TiO_2

microcapsules is due to the CO_2 supercritical drying treatment. In CO_2 supercritical drying, the organic part of the surface was largely dehydrated, whereas the inorganic part showed strong resistance to the dehydration. The presence of both components with a certain ratio could contribute to the wrinkled surface of the dried microcapsules. No wrinkle is observed on the surface of ASA microcapsules, indicating the uniform dehydration of the surface. Organic or inorganic compound could be present in the surface with a large ratio. The EDX spectra confirm the presence of silicon and titanium on the surface of the ASA (Figure 1C) and alginate@TiO_2 (Figure 1D) microcapsules, respectively. In the ASA microcapsule, the elemental quantity of calcium is larger than that of silicon (Figure 1C), demonstrating that calcium alginate is a main component of the outmost surface of the ASA microcapsule. This could lead to the uniform dehydration of the microcapsule in drying, which was evidenced by the SEM image (Figure 1A). In the alginate@TiO_2 microcapsule, the EDX spectrum (Figure 1D) indicates that the outmost surface is composed of titania and calcium alginate. The presence of a small amount of calcium alginate in the surface of the alginate@TiO_2 microcapsules could result in the formation of wrinkles on the surface during the CO_2 supercritical drying processes, in accordance with the SEM observation (Figure 1B).

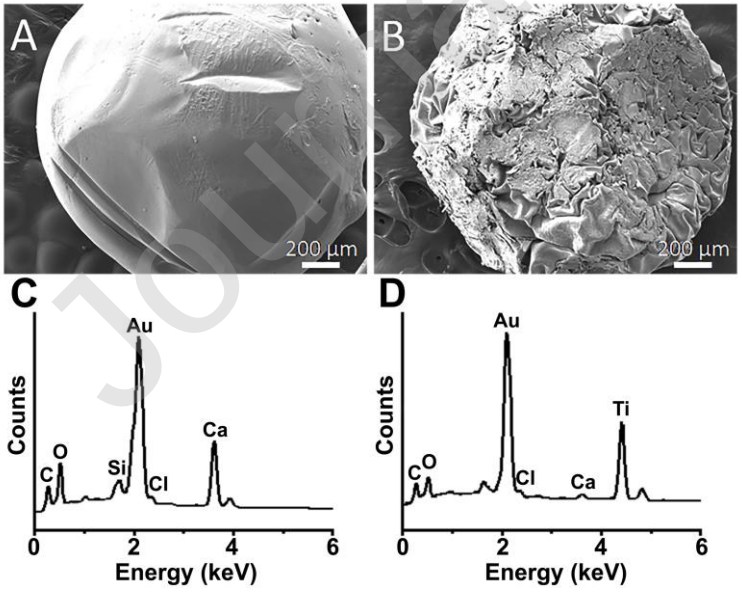

Figure 1. Structure and chemical composition of the microcapsules. SEM micrograph of an ASA microcapsule (A) and an alginate@TiO_2 microcapsule (B). EDX spectrum of the surface of the ASA microcapsule (C) and the alginate@TiO_2 microcapsule (D). All microcapsules were supercritically dried with CO_2 prior to analyses.

***In vivo* experiments.** Our previous studies have demonstrated the high biocompatibility and stability of the cell-laden alginate@TiO_2 microcapsules with the release of metabolic products in *in vitro* condition.[41-42] To approach the practical applications, *in vivo* experiments were performed in this study to evaluate the stability of alginate@TiO_2 microcapsules without or with entrapped cells and their induced immune responses. The immune responses of hosts in this study can be originated from both the pathogen associated molecular patterns of the microcapsules and the immune mediators of the encapsulated cells.[47] The microcapsule-induced immune responses could be revealed based on the comparison between the control group and the alginate@TiO_2 microcapsules without entrapped cells, while the encapsulated cell-induced immune responses would be evidenced on the basis of the comparison between the alginate@TiO_2 microcapsules without entrapped cells and the ones with entrapped cells. In addition, the immune-isolation towards the entrapped cells offered by the alginate@TiO_2 microcapsules will be assessed by the study on the viability and morphology change of the entrapped cells. ASA microcapsules without or with entrapped cells were set as a reference for comparison.[40]

***In vivo* stability of microcapsules.** The *in vivo* stability of all microcapsules without or with entrapped cells was assessed by their recovery rate 2 days and 2 months after implantation (Table S1). 2-day post-implantation, more than 63% of all kinds of microcapsules could be retrieved. They were located in the subcutaneous area where they were initially placed. The incision of back midline for the recovery of microcapsules resulted in the breaken of some microcapsules. Few white residual titania fragments could thus be

found upon the recovery of the implanted alginate@TiO_2 microcapsules. It is important to underline that almost no inflammation sign was detectable two days after implantation. Both alginate@TiO_2 microcapsules and cell-laden ones were thus biocompatible towards the host organism. The recovery rate for alginate@TiO_2 microcapsules and cell-laden ones were 63 and 70%, respectively (Table S1), being slightly lower than that for pure and cells-laden ASA microcapsules which was 77 and 81%, respectively (Table S1). 2-month post-implantation, the percentage of the recovered pure alginate@TiO_2 microcapsules was 57%, which is higher than recovery rate of ASA microcapsules (43%) (Table S1). The recovery rate of cell-laden alginate@TiO_2 microcapsules was 33%, thus being significantly higher than that of cell-laden ASA microcapsules (7%) (Table S1). In general, the recovery rate of the cell-laden ASA and the cell-laden alginate@TiO_2 microcapsules were lower than that of their pure microcapsule counterparts. This could attribute to the presence of encapsulated HepG2 cells which will influence the stability of microcapsules. The cell growth and proliferation or the metabolic secreation of the entrapped cells might loosen the matrix of microcapsules. It is worth to note that around one third of the cell-laden alginate@TiO_2 microcapsules could be recovered in good shape, whereas only 2 of the 30 cell-laden ASA microcapsules were recovered. This directly evidences that the *in vivo* stability of alginate@TiO_2 microcapsules was much higher than that of ASA microcapsules especially after cell encapsulation. The alginate@TiO_2 microcapsules resisted much better to the chemical environment of host organisms, to the internal pressure due to the growth of rats and to the friction due to the movements of host organisms than ASA microcapsules.

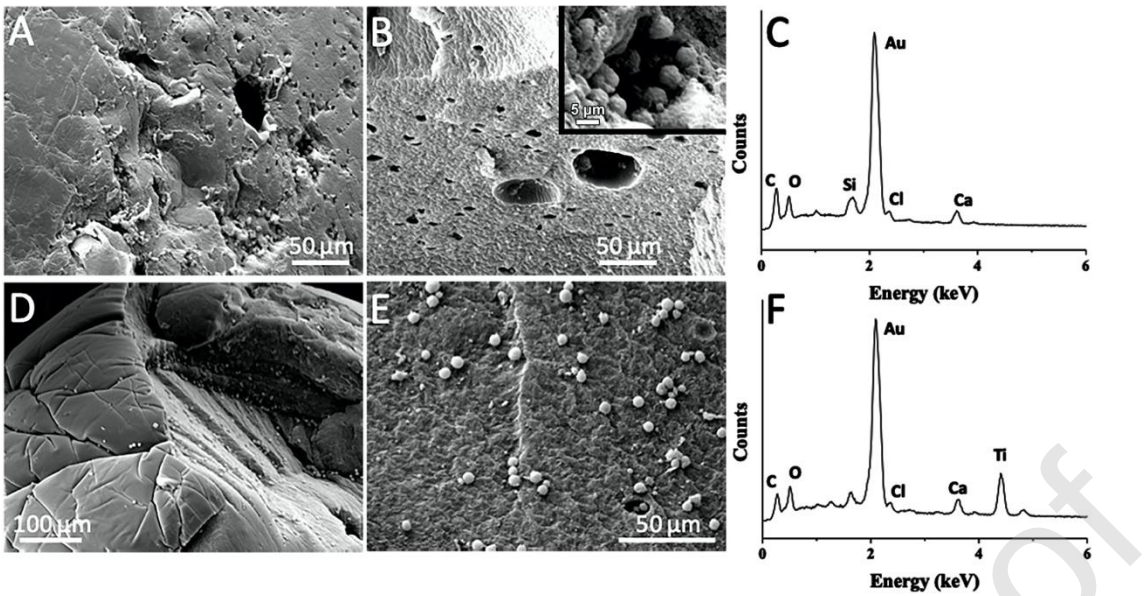

Figure 2. Structure and chemical composition of the cell-laden microcapsules 2-day post-implantation. (A) SEM micrographs of the surface of a cell-laden ASA microcapsule. (B) SEM micrographs of the core of the cell-laden ASA microcapsule and encapsulated cells (inset image). (C) EDX spectrum of the surface of the cell-laden ASA microcapsule. (D) SEM micrographs of the surface of a cell-laden alginate@TiO_2 microcapsule. (E) SEM micrographs of the core of the cell-laden alginate@TiO_2 microcapsule. (F) EDX spectrum of the surface of the cell-laden alginate@TiO_2 microcapsule. All microcapsules were supercritically dried with CO_2 prior to analyses.

In order to trace the changes of the morphology, structure and chemical composition of the microcapsules with time after implantation, cell-laden microcapsules were recovered 2 days after implantation and characterized using SEM and EDX. Some holes can be observed on the surface of the ASA microcapsules (Figure 2A), which indicates the erosion of the ASA microcapsules by chemical environment of host organism, while the morphology of the alginate@TiO_2 microcapsules 2-day post-implantation remains the same as that of the original microcapsule (Figure 2D), only some wrinkles caused by CO_2 supercritical treatment can be observed. In addition, HepG2 cells are homogeneously dispersed in both ASA and

alginate@TiO_2 microcapsules (Inset image in Figure 2B, Figure 2E). The EDX spectrum of the cell-laden alginate@TiO_2 microcapsule (Figure 2F) 2-day post-implantation exhibited very similar elemental distribution with the one performed before implantation (Figure 1D). Compared to the pre-implantation ASA microcapsule (Figure 1C), the EDX spectrum of the ASA microcapsule 2 days after implantation shows that the ratio of Ca Kα signal and Si Kα signal of the microcapsule decreased (Figure 2C), indicating a possible dissolution of the outmost layer of calcium alginate. In the cell-laden alginate@TiO_2 microcapsule, the ratio of Ti Kα signal and Si Kα signal almost maintained during the implantation time, which proves the high chemical stability of the outmost titania layer.

Body weight evolution of rats with implants. The evolution of body weight is a direct parameter to indicate the proper fed and the overall health of animals. The body weight of rats was recorded during two months after implantation. The growth curves and gain ratio of the rat weight are presented in Figure S2 and Table 1, respectively. The weight gain of the rats with implants is similar to that of the control rats (~10%), demonstrating that all kinds of implanted microcapsules would not influence the health state of rats.

Monitoring of the incision site. The scratching of the incision site was daily monitored to assess the possible discomfort induced by implants. If such scratching was observed, astrexine was used to facilitate the healing of wound. Table 1 presents the number and percentage of rats in each experimental group with surgical site irritation.

Table 1. Weight gain ratio of rats 2 months after implantation and use of astrexine in the different experimental groups.

Group	Weight gain ratio	Use of astrexine
Control	9%	3/13 animals (23%)
ASA	7%	2/10 animals (20%)
Alginate@TiO_2	9%	4/10 animals (40%)
Cell-laden ASA	14%	6/11 animals (55%)

Cell-laden alginate@TiO_2	11%	3/10 animals (30%)

In the control group, 3 rats (23%) presented inflamed wounds, and were treated with antiseptic. 2 rats implanted with ASA microcapsules (20%, as similar as the ratio of the control group) show surgical site irritation, indicating less immune responses were induced by ASA microcapsules. It could be attributed to the high biocompatibility of the outmost alginate layer. As a comparison, the cell-laden ASA microcapsules elicited significantly more immune responses that 55% rats presented inflamed wounds. This could be resulted from the immune mediators of the encapsulated cells. The ratio of the rats implanted with the alginate@TiO_2 microcapsules with surgical site irritation was slight higher than the control groups, which demonstrates that very slight immune responses could be induced by the alginate@TiO_2 microcapules. It is worth noting that the number of the rats implanted with the cell-laden alginate@TiO_2 microcapsules with surgical site irritation (3) is similar to that of the rats implanted with the alginate@TiO_2 microcapsules (4), confirming the less significance of the immune responses induced by the immune mediators of the cells encapsulated in the alginate@TiO_2 microcapsules. All above, the observed inflammation was very probably caused by the surgery or the immune mediators of the cells encapsulated in ASA but was not due to the implanted ASA or alginate@TiO_2 microcapsules.

ELISA monitoring of inflammation induced by implantation. Interleukin-6 (IL-6) is a pro-inflammatory cytokine secreted mostly by macrophages to stimulate immune response following an infection or a trauma such as tissue damage. It is a mediator of fever and is involved in the development of many auto-immune diseases (e.g. type 1 *diabetes mellitus*) and its level increases in blood circulation following bacterial infection, for example pneumonia. Monocyte Chemotactic Protein-1 (MCP-1/CCL2) is a cytokine of the CC chemokine family recruiting specific types of leukocytes like monocytes, memory T cells and dendritic cells to the sites of inflammation induced by tissue injury or infection. These two

markers of inflammation have been used in Wistar rats, to assess the possible inflammation induced by the implantation of microcapsules.

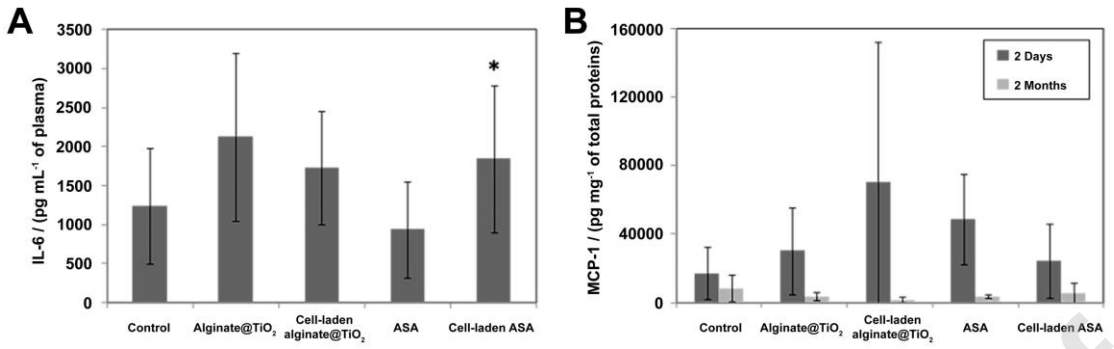

Figure 3. Inflammation induced by implantation. (A) IL-6 concentration in rat blood plasma 2-day post-implantation. *IL-6 concentration in cell-laden ASA microcapsules was greater than that in pure ASA microcapsules ($p < 0.02$). (B) MCP-1 concentration in rat tissue lysate 2-day and 2-month post-implantation.

IL-6 concentration in blood plasma has been assayed 2 days after implantation. As shown in Figure 3A, no significant difference was observed in IL-6 concentration between the control group and the rats with implanted alginate@TiO_2 microcapsules, which demonstrates the high biocompability of the alginate@TiO_2 microcapsules. A slight but statistically significant increase is shown between the rats with implanted ASA microcapsules with and the one with implanted ASA microcapsules without entrapped cells ($p < 0.02$) (Figure 3A), which could be attributed to the immune responses induced by the immune mediators of the encapsulated cells. Please note that the IL-6 concentration of the rats with implanted cell-laden alginate@TiO_2 microcapsules is similar to that with implanted alginate@TiO_2 microcapsules, indicating the less significance of the immune responses induced by the immune mediators of the cells encapsulated in the alginate@TiO_2 microcapsules. MCP-1 concentration was assayed in tissue lysate 2 days and 2 months after implantation (Figure 3B). 2-days post-implantation, no significant difference was observed between the control

group and the other experimental groups, demonstrating that the observed inflammation was highly likely caused by the surgery for the implantation of microcapsules but was not due to the implanted microcapsules. 2-months post-implantation, the MCP-1 concentration of all grouped rats was returned to a basal level and showed no significant difference (Figure 3B). Consequently, the monitoring of these two markers demonstrates that the inflammation induced by the implanted microcapsules is insignifigant, being in agreement with the monitoring experiments of surgical sites. Based on the above results, it could be consolidated again that the observed inflammation was highly probably caused by the surgery or the immune mediators of the cells encapsulated in ASA but was not due to the implanted ASA or alginate@TiO_2 microcapsules.

Histological analysis of implantation. In order to trace the potential inflammation induced by ASA and alginate@TiO_2 microcapsules and their immune isolation towards the entrapped cells, histological sections of the implanted microcapsules without or with entrapped cells and the contacting subcutaneous tissues have been stained and analyzed.

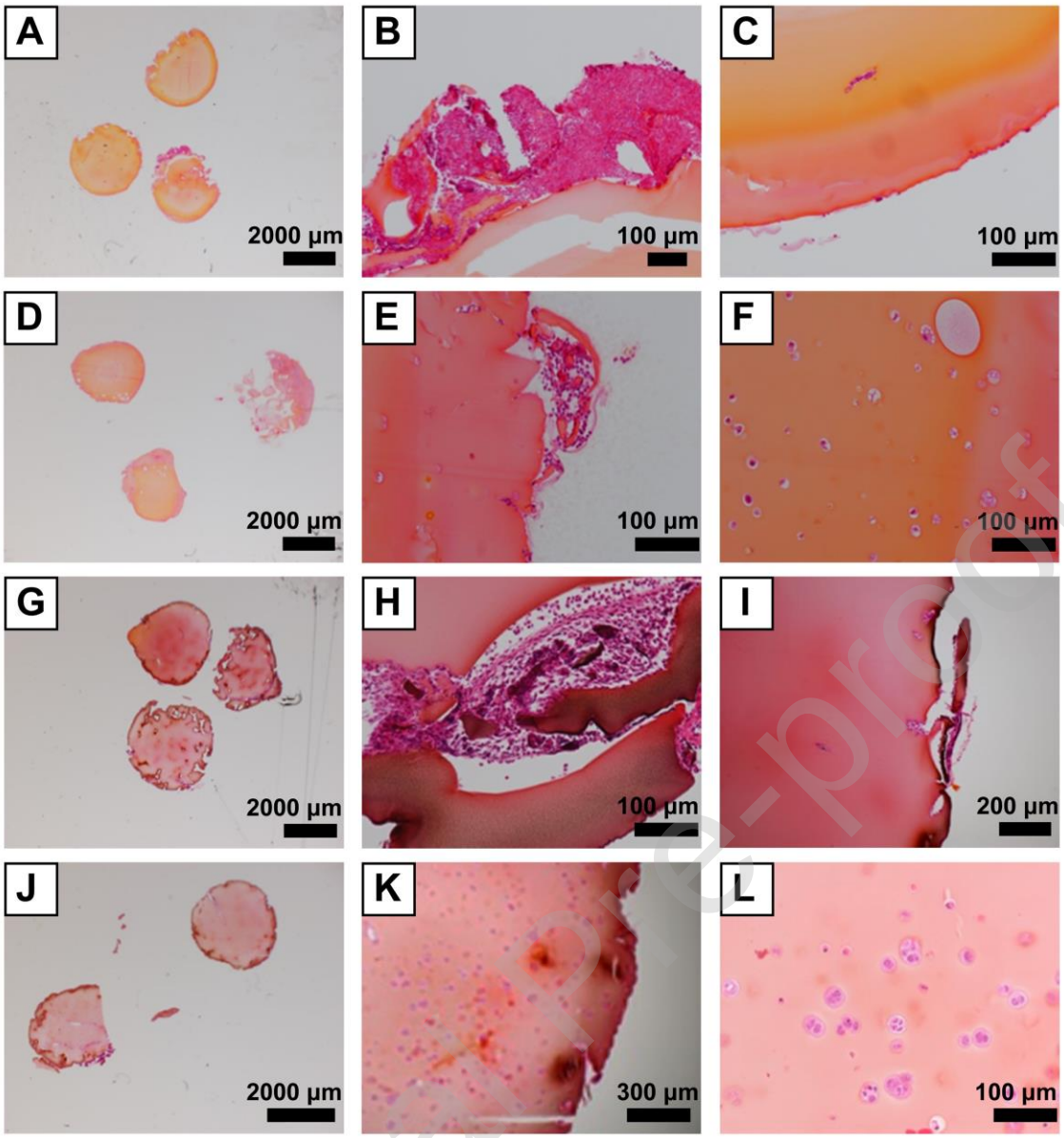

Figure 4. Histological sections of implanted microcapsules. (A-C) Histological sections of ASA microcapsules 2-day post-implantation. (D-F) Histological sections of cell-laden ASA microcapsules 2-day post-implantation. (G-I) Histological sections of alginate@TiO_2 microcapsules 2-day post-implantation. (J-L) Histological sections of cell-laden alginate@TiO_2 microcapsules 2-day post-implantation.

The histological sections of entire implanted ASA microcapsules (Figure 4A), alginate@TiO_2 microcapsules (Figure 4G), and cell-laden alginate@TiO_2 microcapsules (Figure 4J) indicate that their spherical morphology could be maintained after implantation,

evidencing their *in vivo* stability. One of the cell-laden ASA microcapsules was almost totally broken (Figure 4D), probably because the growth or metabolism of entrapped cells decreased the stability of ASA microcapsules. Focusing on the surface of implanted microcapsules, some eroded portions were observed in a ASA microcapsule (Figure 4B), a cell-laden ASA microcapsule (Figure 4E), and an alginate@TiO_2 microcapsule (Figure 4H), on which the host cells could embed and colonize easily, whereas a cell-laden alginate@TiO_2 microcapsule showed an intact surface where no or few cells were deposited (Figure 4K). The host cells did not invade into the core part of the ASA (Figure 4C) and alginate@TiO_2 (Figure 4I) microcapsules, proving their immune-isolation. The viability of the cells entrapped in the ASA and alginate@TiO_2 microcapsules were assessed by their morphology change. Most of the cells entrapped in the ASA microcapsules display a condensed nucleus and a volume-reduced cytoplasm in comparison to the size of the voids initially formed, suggesting their non-viability (Figure 4F). In the cell-laden alginate@TiO_2 microcapsules, the entrapped cells maintained their original morphology with a well-defined nucleus and cytoplasm, indicative of their high viability (Figure 4L). Overall, alginate@TiO_2 microcapsules not only present a high *in vivo* stability to maintain their spheric morphology, but also offer a biocompatible environment for the entrapped cells, which makes them a promising material to encapsulate cells for cell therapy.

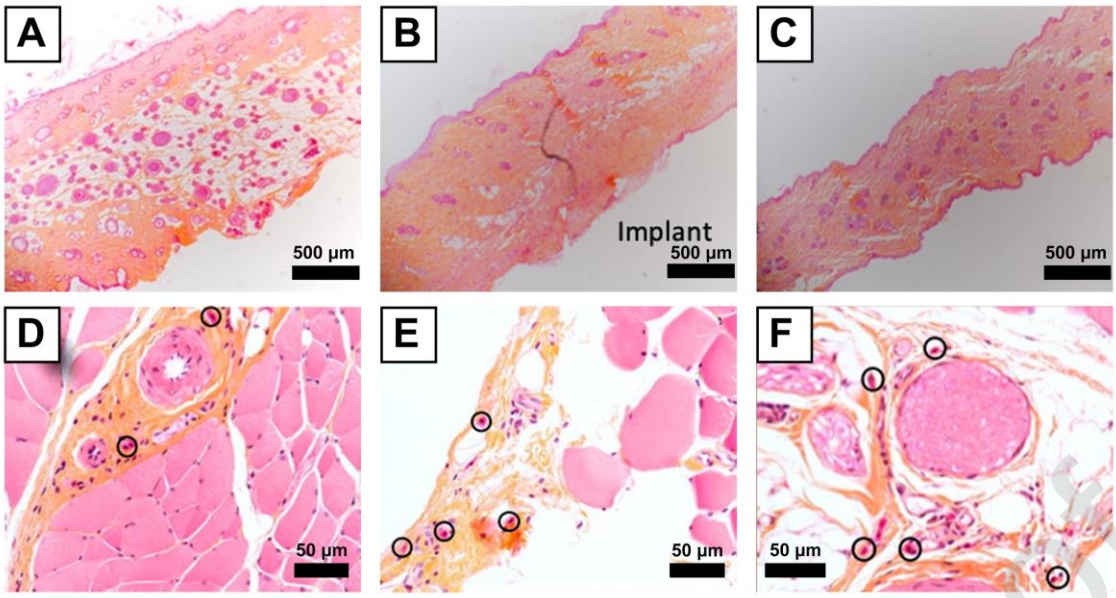

Figure 5. Histological sections of microcapsule-contacting subcutaneous tissues. (A) Histological sections of tissues in the surgical site of the control rats 2-day post-implantation. (B) Histological sections of ASA microcapsule-contacting tissues 2-day post-implantation. (C) Histological sections of alginate@TiO_2 microcapsule-contacting tissues 2-day post-implantation. (D) Histological sections of tissues in the surgical site of the control rats 2-month post-implantation. (E) Histological sections of cell-laden ASA microcapsule-contacting tissues 2-month post-implantation. (F) Histological sections of cell-laden alginate@TiO_2 microcapsule-contacting tissues 2-month post-implantation.

Histological sections of microcapsule-contacting tissues were characterized to trace the possible inflammation induced by the implantation of microcapsules. Almost no or very few inflammatory response was observed in the histological sections of tissues in all experimental grouped rats 2-day post-implantation (Figure 5A, 5B, 5C), which are consistent with the results analyzed by and the IL-6 (Figure 3A) and MCP-1 concentration (Figure 3B). 2-month post-implantation, several mast cells could be found near blood vessels in all experimental grouped rats, which were recognized by their purple nucleus surrounded by red staining and indicated by black circles in the micrographs (Figure 5D, 5E, 5F). Mast cells are sentinel

cells mostly found near blood vessels in normal tissue. Large quantities of mast cells present further away from blood vessels could be a signal of rejection. In our case, no mast cells could be seen in the surrounding muscles, demonstrating almost no inflammation of both control rats and the rats with implanted microcapsules and thus evidencing the high biocompatibility of all *in vivo* used microcapsules.

Viability of the entrapped cells in implanted microcapsules. The viability of entrapped cells was evaluated by fluorescein diacetate (FDA), in order to verify the protection and immune isolation of microcapsules. FDA shows green fluorescence when reacting with active intracellular esterases in cytoplasm and attribute a green stain to living cells observed by fluorescent microscopy.

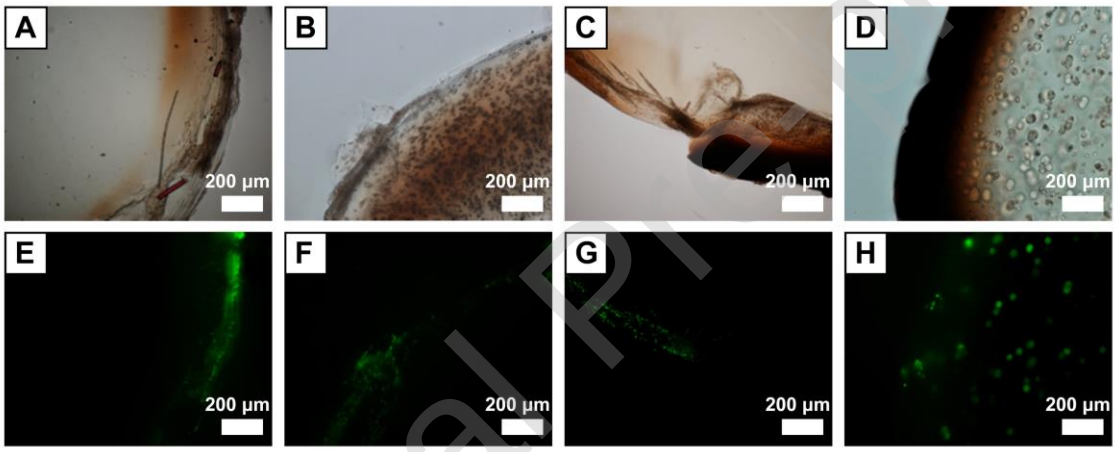

Figure 6. Viability of the entrapped cells in implanted microcapsules. (A, E) Micrographs of the FDA-stained ASA microcapsule captured in bright filed (A) and in green fluorescent channel (E) 2-day post-implantation. (B, F) Micrographs of the FDA-stained implanted cell-laden ASA microcapsule captured in bright filed (B) and in green fluorescent channel (F) 2-day post-implantation. (C, G) Micrographs of the FDA-stained implanted alginate@TiO_2 microcapsule captured in bright filed (C) and in green fluorescent channel (G) 2-day post-implantation. (D, H) Micrographs of the FDA-stained implanted cell-laden alginate@TiO_2 microcapsule captured in bright filed (D) and in green fluorescent channel (H) 2-day post-implantation.

As shown in Figure 6A and 6E, a pure ASA microcapsule displays green fluorescence on the outmost layer of the microcapsules, indicating the deposition of host cells on the microcapsule shell. Compared to the ASA microcapsule, weaker green fluorescence was observed in the outmost layer of alginate@TiO_2 microcapsules (Figure 6C and 6G), which demonstrates less cell deposition occurred on the surface of the alginate@TiO_2 microcapsules. These results evidence that alginate@TiO_2 microcapsules possess higher resistance against cell invasion than the ASA microcapsules.

Figure 6B and 6F present that the entrapped cells in an ASA microcapsule showed no sign of viability 2-day post-implantation, which correlates with abnormal cell morphology observed in the micrograph of histological section (Figure 4F). Figure 6D and 6H highlight very high viability of the entrapped cells in the alginate@TiO_2 microcapsules 2-day post-implantation, which fits the observation of the "normal" cell morphology in histological section (Figure 4L). These results suggest more efficient *in vivo* immune-isolation of the alginate@TiO_2 microcapsules than that of the ASA microcapsules, confirming their ability to serve as a promising cell reservoir for cell therapy.

4. CONCLUSIONS AND PERSPECTIVES

The alginate@TiO_2 hybrid microcapsules show high *in vivo* biocompatibility, high *in vivo* stabilty and can provide entrapped cells with highly efficient immune-isolation. The morphology, structure, and chemical composition of these two kinds of microcapsules were investigated. Compared to ASA microcapsules used as a reference group, alginate@TiO_2 microcapsules demonstrated much higher *in vivo* stability, which was indicated by their unchanged chemical composition after implantation. The *in vivo* biocompatibility of the microcapsules and the potentially induced inflammation or rejection were assessed by a quantification of IL-6 concentration in rat blood plasm, MCP-1 concentration in rat tissue lysates, histological sections of the microcapsules and tissue in direct contact. Both hybrid

microcapsules showed excellent biocompatibility to the hosts and insignificant inflammations. The immune-isolation of the microcapsules was investigated by estimating the viability of the entrapped cells after implantation. Much higher viability was observed in the entrapped cells in alginate@TiO_2 microcapsule, which confirmed these hybrid microcapsules provided more efficient immune-isolation and protection to the encapsulated cells. The alginate@TiO_2 hybrid microcapsules present such high *in vivo* stability, high resistance to the chemical environment of host organisms, high *in vivo* biocompatibility, and excellent immune-isolation, which makes them a very promising material for cell therapy.

Although the *in vivo* biocompatibility and stability of the alginate@TiO_2 hybrid microcapsules have been proven in this study, several challenges still remain in the way to their further practical cell therapy applications. 1) The microcaspules only work as a reservoir for the encapsulated cells, thus can not induce bioaugementation to maximize the activity or viability of the encapsulated cells. More additives could be considered in the design of the microcapsules to optimise the cell viability or boost the cell activity. 2) HepG2 cells is the model cells used in the study, which shows no therapeutic function. More Functional cells should be used and investigated in the alginate@TiO_2 microcapsules instead of HepG2 cells for target diseases. 3) The fundamental mechanism of the immune responses elicited by the alginate@TiO_2 microcapsules has not yet clearly uncovered. This mechanism should be deeply and systematically explored, which would be very significant for the design guidence of implanted materials for cell therapy. Finally the long term immune compatibility of alginate@TiO_2 microcapsules will be deeply studied in our forthcoming work.

AUTHOR INFORMATION

Credit author statement

Grégory Leroux: Conceptualization, Methodology, Validation, Investigation, Writing-Original Draft. **Myriam Neumann:** Formal analysis, Validation, Writing-Original Draft. **Christophe F. Meunier:** Methodology, Formal analysis, Investigation. **Virginie Voisin:** Investigation, Validation. **Isabelle Habsch:** Investigation, Validation. **Nathalie Caron:** Resources. **Carine Michiels:** Resources, Supervision. **Li Wang:** Investigation, Formal analysis, Writing-Original Draft, Writing-Review & Editing, Visualization. **Bao-Lian Su:** Conceptualization, Writing-Review & Editing, Project administration.

CONFLICT OF INTEREST

The authors declare no competing financial interest.

ACKNOWLEDGMENT

This work was supported by Program for Changjiang Scholars and Innovative Research Team in University (IRT_15R52) and "Algae Factory" (1610187) European H2020 program financed by FEDER and Wallonia Region of Belgium. G. Leroux thanks the University of Namur for his assistant position to realize his PhD research. We are grateful to Laetitia Giordano and Vanessa Colombaro of URPhyM for their help and advices on animal experiments. We thank Prof. Yves Poumay, Daniel Van Vlaender and Valérie De Glas of LabCeTi for their support in histological techniques and examination. The present work is in accordance with the rules of the National Institutes of Health Guide for the Care and Use of Laboratory Animals and the project was approved by the Committee on the Ethics of Animal Experiments of the University of Namur.

REFERENCES

1. Forbes, S. J.; Rosenthal, N., Preparing the ground for tissue regeneration: from mechanism to therapy. *Nat. Med.* **2014**, 20 (8), 857.

2. Fliervoet, L. A.; Mastrobattista, E., Drug delivery with living cells. *Adv. Drug Delivery. Rev.* **2016**, 106, 63-72.

3. Trounson, A.; McDonald, C., Stem cell therapies in clinical trials: progress and challenges. *Cell Stem Cell* **2015**, 17 (1), 11-22.

4. Okano, H.; Nakamura, M.; Yoshida, K.; Okada, Y.; Tsuji, O.; Nori, S.; Ikeda, E.; Yamanaka, S.; Miura, K., Steps toward safe cell therapy using induced pluripotent stem cells. *Circ. Res.* **2013**, 112 (3), 523-533.

5. Stuckey, D. W.; Shah, K., Stem cell-based therapies for cancer treatment: separating hope from hype. *Nat. Rev. Cancer* **2014**, 14 (10), 683.

6. Ludwig, B.; Rotem, A.; Schmid, J.; Weir, G. C.; Colton, C. K.; Brendel, M. D.; Neufeld, T.; Block, N. L.; Yavriyants, K.; Steffen, A., Improvement of islet function in a bioartificial pancreas by enhanced oxygen supply and growth hormone releasing hormone agonist. *Proc. Natl. Acad. Sci. USA* **2012**, 109 (13), 5022-5027.

7. Leonard, A.; Dandoy, P.; Danloy, E.; Leroux, G.; Meunier, C. F.; Rooke, J. C.; Su, B.-L., Whole-cell based hybrid materials for green energy production, environmental remediation and smart cell-therapy. *Chem. Soc. Rev.* **2011**, 40 (2), 860-885.

8. Su, B. L.; Sanchez, C.; Yang, X. Y., Hierarchically structured porous materials: from nanoscience to catalysis, separation, optics, energy, and life science. *John Wiley & Sons:* **2012**.

9. Sun, M. H.; Huang, S. Z.; Chen, L. H.; Li, Y.; Yang, X. Y.; Yuan, Z. Y.; Su, B. L., Applications of hierarchically structured porous materials from energy storage and conversion, catalysis, photocatalysis, adsorption, separation, and sensing to biomedicine. *Chem. Soc. Rev.* **2016**, 45 (12), 3479-3563.

10. Geng, W.; Wang, L.; Jiang, N.; Cao, J.; Xiao, Y.-X.; Wei, H.; Yetisen, A. K.; Yang, X.-Y.; Su, B.-L., Single-cells in nanoshells for functionalization of living cells. *Nanoscale* **2018**, 10 (7), 3112-3129.

11. Desai, T.; Shea, L. D., Advances in islet encapsulation technologies. *Nat. Rev. Drug Discov.* **2017**, 16 (5), 338.

12. Chang, R.; Faleo, G.; Russ, H. A.; Parent, A. V.; Elledge, S. K.; Bernards, D. A.; Allen, J. L.; Villanueva, K.; Hebrok, M.; Tang, Q., Nanoporous immunoprotective device for stem-cell-derived β-cell replacement therapy. *ACS Nano* **2017**, 11 (8), 7747-7757.

13. Nyitray, C. E.; Chang, R.; Faleo, G.; Lance, K. D.; Bernards, D. A.; Tang, Q.; Desai, T. A., Polycaprolactone thin-film micro-and nanoporous cell-encapsulation devices. *ACS Nano* **2015**, 9 (6), 5675-5682.

14. Seliktar, D., Designing cell-compatible hydrogels for biomedical applications. *Science* **2012**, 336 (6085), 1124-1128.

15. Ellis, C.; Ramzy, A.; Kieffer, T. J., Regenerative medicine and cell-based approaches to restore pancreatic function. *Nat. Rev. Gastroenterol. Hepatol.* **2017**, 14 (10), 612.

16. Liu, Z.; Tang, M.; Zhao, J.; Chai, R.; Kang, J., Looking into the future: toward advanced 3D biomaterials for stem-cell-based regenerative medicine. *Adv. Mater.* **2018**, 1705388.

17. Wang, L.; Neumann, M.; Fu, T.; Li, W.; Cheng, X.; Su, B. L., Porous and responsive hydrogels for cell therapy. *Curr. Opin. Colloid Interface Sci.* **2018**, 38, 135-157.

18. Burdick, J. A.; Mauck, R. L.; Gerecht, S., To serve and protect: hydrogels to improve stem cell-based therapies. *Cell Stem Cell* **2016**, 18 (1), 13-15.

19. Li, J.; Mooney, D. J., Designing hydrogels for controlled drug delivery. *Nat. Rev. Mater.* **2016**, 1 (12), 16071.

20. Lee, K. Y.; Mooney, D. J., Alginate: properties and biomedical applications. *Prog. Polym. Sci.* **2012**, 37 (1), 106-126.

21. Sun, J.; Tan, H., Alginate-based biomaterials for regenerative medicine applications. *Materials* **2013**, 6 (4), 1285.

22. Meunier, C. F.; Dandoy, P.; Su, B. L., Encapsulation of cells within silica matrixes: Towards a new advance in the conception of living hybrid materials. *J. Colloid Interface Sci.* **2010**, 342 (2), 211-224.

23. Rooke, J. C.; Léonard, A.; Sarmento, H.; Meunier, C. F.; Descy, J. P.; Su, B. L., Novel photosynthetic CO_2 bioconvertor based on green algae entrapped in low-sodium silica gels. *J. Mater. Chem.* **2011**, 21 (4), 951-959.

24. Yang, S. H.; Ko, E. H.; Choi, I. S., Cytocompatible encapsulation of individual Chlorella cells within titanium dioxide shells by a designed catalytic peptide. *Langmuir* **2011**, 28 (4), 2151-2155.

25. Rooke, J. C.; Vandoorne, B.; Léonard, A.; Meunier, C. F.; Cambier, P.; Sarmento, H.; Descy, J. P.; Su, B. L., Prolonging the lifetime and activity of silica immobilised Cyanidium caldarium. *J. Colloid Interface Sci.* **2011**, 356 (1), 159-164.

26. Youn, W.; Ko, E. H.; Kim, M.-H.; Park, M.; Hong, D.; Seisenbaeva, G. A.; Kessler, V. G.; Choi, I. S., Cytoprotective encapsulation of individual Jurkat T cells within durable TiO_2 shells for T cell therapy. *Angew. Chem. In. Ed.* **2017**, 56 (36), 10702-10706.

27. Bhatia, R. B.; Brinker, C. J.; Gupta, A. K.; Singh, A. K., Aqueous sol-gel process for protein encapsulation. *Chem. Mater.* **2000**, 12 (8), 2434-2441.

28. Meunier, C. F.; Rooke, J. C.; Hajdu, K.; Van Cutsem, P.; Cambier, P.; Léonard, A.; Su, B. L., Insight into cellular response of plant cells confined within silica-based matrices. *Langmuir* **2010**, 26 (9), 6568-6575.

29. Li, Y.; Xiao, Y.; Liu, C., The horizon of materiobiology: a perspective on material-guided cell behaviors and tissue engineering. *Chem. Rev.* **2017**, 117 (5), 4376-4421.

30. Jiang, N.; Yang, X. Y.; Deng, Z.; Wang, L.; Hu, Z. Y.; Tian, G.; Ying, G. L.; Shen, L.; Zhang, M. X.; Su, B. L., A stable, reusable, and highly active photosynthetic bioreactor

by bio-interfacing an individual cyanobacterium with a mesoporous bilayer nanoshell. *Small* **2015**, 11 (17), 2003-2010.

31. Wang, L.; Li, Y.; Yang, X. Y.; Zhang, B. B.; Ninane, N.; Busscher, H. J.; Hu, Z. Y.; Delneuville, C.; Jiang, N.; Xie, H.; Van Tendeloo, G.; Hasan, T.; Su, B. L., Single-cell yolk-shell nanoencapsulation for long-term viability with size-dependent permeability and molecular recognition. *Natl. Sci. Rev.* **2020**, nwaa097.

32. Mehrali, M.; Thakur, A.; Pennisi, C. P.; Talebian, S.; Arpanaei, A.; Nikkhah, M.; Dolatshahi- Pirouz, A., Nanoreinforced hydrogels for tissue engineering: biomaterials that are compatible with load-bearing and electroactive tissues. *Adv. Mater.* **2017**, 29 (8), 1603612.

33. Heinemann, S.; Heinemann, C.; Wenisch, S.; Alt, V.; Worch, H.; Hanke, T., Calcium phosphate phases integrated in silica/collagen nanocomposite xerogels enhance the bioactivity and ultimately manipulate the osteoblast/osteoclast ratio in a human co-culture model. *Acta Biomater.* **2013**, 9 (1), 4878-4888.

34. Baumann, B.; Wittig, R.; Lindén, M., Mesoporous silica nanoparticles in injectable hydrogels: factors influencing cellular uptake and viability. *Nanoscale* **2017**, 9 (34), 12379-12390.

35. Coradin, T.; Nassif, N.; Livage, J., Silica–alginate composites for microencapsulation. *Appl. Microbiol. Biotechnol.* **2003**, 61 (5-6), 429-434.

36. Zhang, B. B.; Wang, L.; Charles, V. R.; Rooke, J. C.; Su, B. L., Robust and biocompatible hybrid matrix with controllable permeability for microalgae encapsulation. *ACS Appl. Mater. Interf.* **2016**, 8 (14), 8939-8946.

37. Dandoy, P.; Meunier, C. F.; Michiels, C.; Su, B. L., Hybrid shell engineering of animal cells for immune protections and regulation of drug delivery: towards the design of "artificial organs". *PLoS One* **2011**, 6 (6), e20983.

38. Desmet, J.; Meunier, C. F.; Danloy, E. P.; Duprez, M.-E.; Hantson, A.-L.; Thomas, D.; Cambier, P.; Rooke, J. C.; Su, B.-L., Green and sustainable production of high value compounds via a microalgae encapsulation technology that relies on CO_2 as a principle reactant. *J. Mater. Chem. A* **2014**, 2 (48), 20560-20569.

39. Desmet, J.; Meunier, C.; Danloy, E.; Duprez, M.-E.; Lox, F.; Thomas, D.; Hantson, A.-L.; Crine, M.; Toye, D.; Rooke, J., Highly efficient, long life, reusable and robust photosynthetic hybrid core-shell beads for the sustainable production of high value compounds. *J. Colloid Interface Sci.* **2015**, 448, 79-87.

40. Dandoy, P.; Meunier, C. F.; Leroux, G.; Voisin, V.; Giordano, L.; Caron, N.; Michiels, C.; Su, B. L., A hybrid assembly by encapsulation of human cells within mineralised beads for cell therapy. *PLoS One* **2013**, 8 (1), e54683.

41. Leroux, G.; Neumann, M.; Meunier, C. F.; Fattaccioli, A.; Michiels, C.; Arnould, T.; Wang, L.; Su, B. L., Hybrid alginate@TiO_2 porous microcapsules as a reservoir of animal cells for cell therapy. *ACS Appl. Mater. Interf.* **2018**, 10 (44), 37865-37877.

42. Leroux, G.; Neumann, M.; Meunier, C. F.; Michiels, C.; Wang, L.; Su, B. L., Alginate@TiO_2 hybrid microcapsules as a reservoir of beta INS-1E cells with controlled insulin delivery. *J. Mater. Sci.* **2020**, 55, 7857-7869.

43. Trindade, R.; Albrektsson, T.; Galli, S.; Prgomet, Z.; Tengvall, P.; Wennerberg, A., Osseointegration and foreign body reaction: Titanium implantsactivate the immune system and suppress bone resorptionduring the first 4 weeks after implantation. *Clin. Implant Dent. Relat. Res.* **2018**, 20, 82-91.

44. Chen, Q.; Wang, N.; Zhu, M.; Lu, J.; Zhong, H.; Xue, X.; Guo, S.; Li, M.; Wei, X.; Tao, Y.; Yin, H., TiO_2 nanoparticles cause mitochondrial dysfunction, activate inflammatory responses, and attenuate phagocytosis in macrophages: A proteomic and metabolomic insight. *Redox Biol.* **2018**, 15, 266-276.

45. Yang, H.; Yu, M.; Wang, R.; Li, B.; Zhao, X.; Hao, Y.; Guo, Z.; Han, Y., Hydrothermally grown TiO_2-nanorods on surface mechanical attrition treated Ti: Improved corrosion fatigue and osteogenesis. *Acta Biomater*. **2020**, 116, 400-414.

46. De Vos, P.; Spasojevic, M.; de Haan, B. J.; Faas, M. M., The association between *in vivo* physicochemical changes and inflammatory responses against alginate based microcapsules. *Biomaterials* **2012**, 33 (22), 5552-5559.

47. Ashimova, A.; Yegorov, S.; Negmetzhanov, B.; Hortelano, G., Cell encapsulation within alginate microcapsules: immunological challenges and outlook. *Front. Bioeng. Biotechnol.* **2019**, 7, 380.